Available online at www.sciencedirect.com
SCIENCE DIRECT®
Optical Materials 23 (2003) 403–408
OPTICAL Materials
www.elsevier.com/locate/optmat

Crystal orientation dependence of piezoelectric properties in $LiNbO_3$ and $LiTaO_3$

Wang Yue [a,*], Jiang Yi-jian [b]

[a] College of Applied Science, Beijing Polytechnic University, Beijing, 100022, PR China
[b] National Center of Laser Technology, Beijing Polytechnic University, Beijing 100022, PR China

Abstract

In this paper, the crystal orientation dependence of the piezoelectric properties has been calculated phenomenologically for lithium niobate ($LiNbO_3$) and lithium tantalate ($LiTaO_3$) in three-dimensional space by means of coordinate transformations. The maximum longitudinal piezoelectric constant d_{33} and electromechanical factor k_{33} have been determined. For $LiNbO_3$, the max $d_{33} = 39.60$ pC/N and max $k_{33} = 0.60$ are found at 61.8° and 57.0°, respectively. These angles are canted from the Z-axis to the right in the YOZ mirror plane. The respective values of d_{33} and k_{33} are 6.6 and 3.7 times larger than those alone the Z-axis. For $LiTaO_3$, the max $d_{33} = 14.60$ pC/N and max $k_{33} = 0.32$ are found at 56.8° and 53.5°, respectively. These angles are canted from the Z-axis to the right in the YOZ mirror plane. The respective values of d_{33} and k_{33} are 1.8 and 1.6 times larger than those alone the Z-axis. This suggests that by adopting the optimal directions, the piezoelectric properties of the devices made from $LiNbO_3$ and $LiTaO_3$ crystals and thin films can be greatly enhanced.

Keywords: Lithium niobate; Lithium tantalate; Coordinate transformations; Piezoelectric constants; Electromechanical coupling factors

1. Introduction

Lithium niobate ($LiNbO_3$) and lithium tantalate ($LiTaO_3$) have been the objects of intensive study because of their large piezoelectric effect, optical non-linearties and corresponding potential device in producing sensors, transducers, actuators, electrooptic modulators, memory elements, harmonic generators, etc. [1–7]. Both compounds are ferroelectric at room temperature and may be grown in the form of large optical-quality single crystals. They are uniaxial at all temperatures, with only a single structural phase transition.

In acoustic applications, large piezoelectric constants and electromechanical coupling factors are preferred. It was previously reported that the electrical properties such as dielectric constant, pyroelectric coefficient, piezoelectric and electromechanical coupling factor could be improved by preferentially controlling orientations [8–12].

In this paper, an investigation has been made into enhancing the electromechanical properties by calculating the crystal orientation dependence of the piezoelectric properties of $LiNbO_3$ and $LiTaO_3$. These results will be of benefit for developing further applications of piezoelectricity.

* Corresponding author.

0925-3467/03/$ - see front matter © 2003 Published by Elsevier Science B.V.
doi:10.1016/S0925-3467(02)00328-2

2. Theoretical background

In the ferroelectric phase both $LiNbO_3$ and $LiTaO_3$ exhibit threefold rotation symmetry about the c-axis (i.e. the spontaneous polarization direction). Thus they are members of the trigonal crystal system. In addition, they exhibit mirror symmetry about three planes that are 60° apart and intersect forming a threefold rotation axis. These two symmetry operations classify $LiNbO_3$ and $LiTaO_3$ as members of the 3 m point group.

In the trigonal crystal system, crystals can be structurally characterized by either a hexagonal or rhombohedral unit cell. The coordinate system used to describe the physical tensor properties of $LiNbO_3$ and $LiTaO_3$ is neither hexagonal nor rhombohedral but rather a Cartesian XYZ system. The accepted conventional coordinate system can be chosen as follows: the Z-axis is along the c-axis, the X-axis is perpendicular to the mirror plane and the Y-axis is chosen to form a right-hand system. Thus, the Y-axis must lie in a plane of mirror symmetry [2,3,7].

In order to investigate the crystal orientation dependence of the piezoelectric properties, the transformations of the dielectric stiffness, piezoelectric constants, and elastic compliances from one orientation to another orientation should be considered, which corresponds to a rotation of the axes system. The coordinate transformation process can be defined as follows: first, rotation through a clockwise angle φ about the Z-axis, the original coordinates XYZ can be changed to a set of new coordinates $X'Y'Z'$ ($Z'//Z$), secondly, rotation through a clockwise angle θ about the X'-axis, the coordinate system $X'Y'Z'$ can be changed to another set of new coordinates $X''Y''Z''$ ($X''//X'$). According to the process, the value distribution of these physical quantities can be discussed in arbitrary orientations [13,14].

For a clockwise rotation of the coordinate axes through an angle φ about the Z-axis, the transformation matrix is:

$$A_z = \begin{bmatrix} \cos\varphi & \sin\varphi & 0 \\ -\sin\varphi & \cos\varphi & 0 \\ 0 & 0 & 1 \end{bmatrix} \tag{1}$$

For a clockwise rotation of the coordinate axes through an angle θ about the X-axis, the transformation matrix is:

$$A_x = \begin{bmatrix} 1 & 0 & 0 \\ 0 & \cos\theta & \sin\theta \\ 0 & -\sin\theta & \cos\theta \end{bmatrix} \tag{2}$$

The transformation rules of second, third, fourth rank tensors, respectively, to the dielectric, piezoelectric, and elastic constants can be applied [13,14]. Ref. [3] provides all the formulas to calculate the constants in the new axis system. To simplify the calculation, a compressed notation is used. For the compressed notation, the constants in the new axis system can be calculated by:

$$\varepsilon' = A_x \cdot A_z \cdot \varepsilon \cdot A_z^{t} \cdot A_x^{t} \tag{3}$$

$$d' = A_x \cdot A_z \cdot d \cdot N_z^{t} \cdot N_x^{t} \tag{4}$$

$$s' = N_x \cdot N_z \cdot s \cdot N_z^{t} \cdot N_x^{t} \tag{5}$$

$$N = \begin{bmatrix} a_{11}^2 & a_{12}^2 & a_{13}^2 & a_{12}a_{13} & a_{13}a_{11} & a_{11}a_{12} \\ a_{21}^2 & a_{22}^2 & a_{23}^2 & a_{22}a_{23} & a_{23}a_{21} & a_{21}a_{22} \\ a_{31}^2 & a_{32}^2 & a_{33}^2 & a_{32}a_{33} & a_{33}a_{31} & a_{31}a_{32} \\ 2a_{21}a_{31} & 2a_{22}a_{32} & 2a_{23}a_{33} & a_{22}a_{33}+a_{32}a_{23} & a_{23}a_{31}+a_{33}a_{21} & a_{21}a_{32}+a_{31}a_{22} \\ 2a_{31}a_{11} & 2a_{32}a_{12} & 2a_{33}a_{13} & a_{32}a_{13}+a_{12}a_{33} & a_{33}a_{11}+a_{13}a_{31} & a_{31}a_{12}+a_{11}a_{32} \\ 2a_{11}a_{21} & 2a_{12}a_{22} & 2a_{13}a_{23} & a_{12}a_{23}+a_{22}a_{13} & a_{13}a_{21}+a_{23}a_{11} & a_{11}a_{22}+a_{21}a_{12} \end{bmatrix} \tag{6}$$

N is the bond strain transformation matrix in Ref. [14]. In Eq. (6), $a_{ij} = A_{ij}$, the i, the row and j, the column element in matrix A. The symbol 't' represents 'inversion'.

Table 1
Dielectric constants, compliances (10^{-12} m^2/N) and piezoelectric constants (pC/N) of $LiNbO_3$ and $LiTaO_3$ crystals

Crystal	ε_{11}^{T}	ε_{33}^{T}	s_{11}^{E}	s_{12}^{E}	s_{13}^{E}	s_{14}^{E}	s_{33}^{E}	s_{44}^{E}	d_{15}	d_{22}	d_{31}	d_{33}
$LiNbO_3$	84	30	5.78	−1.01	−1.47	−1.02	5.02	17.0	68	21	−1	6.2
$LiTaO_3$	51	45	4.87	−0.58	−1.25	0.64	4.36	10.8	26	7	−2	8

As a result, the orientation dependence of the longitudinal piezoelectric coefficient d_{33} and electromechanical coupling factor k_{33} and the transverse piezoelectric coefficient d_{31} and electromechanical couple factor k_{31} in three-dimensional space can be determined. The values of k_{33} and k_{31} in the new orientation are calculated as:

$$k_{33}'^2 = \frac{d_{33}'^2}{\varepsilon_{33}'^{T} \cdot s_{33}'^{E}} \tag{7}$$

$$k_{31}'^2 = \frac{d_{31}'^2}{\varepsilon_{33}'^{T} \cdot s_{11}'^{E}} \tag{8}$$

The dielectric constants under constant stress, elastic compliances under constant electric field and piezoelectric constants of $LiNbO_3$ and $LiTaO_3$ can be found from Ref. [2], and they are summarized in Table 1.

3. Results of the calculation

The calculation results for $LiNbO_3$ and $LiTaO_3$ are shown in Figs. 1–4. In the calculations, the values of d_{33}, k_{33}, d_{31} and k_{31} exhibit the relations below:

$$\begin{aligned} d_{33}(\theta+\pi,\varphi+\pi) &= -d_{33}(\theta,\varphi), \\ k_{33}(\theta+\pi,\varphi+\pi) &= -k_{33}(\theta,\varphi) \end{aligned} \tag{9}$$

$$\begin{aligned} d_{31}(\theta+\pi,\varphi+\pi) &= -d_{31}(\theta,\varphi), \\ k_{31}(\theta+\pi,\varphi+\pi) &= -k_{31}(\theta,\varphi) \end{aligned} \tag{10}$$

where $0 \leqslant \theta \leqslant \pi$ and $0 \leqslant \varphi \leqslant 2\pi$. Thus, in these figures, the distance between the origin and a point on the graph represents the absolute value of the constant in the corresponding direction. Figs. 1(a) and 2(a) show the schematic diagrams of the crystal orientation dependence of the longitudinal piezoelectric constant d_{33} and electromechanical coupling factor k_{33} in three-dimensional space,

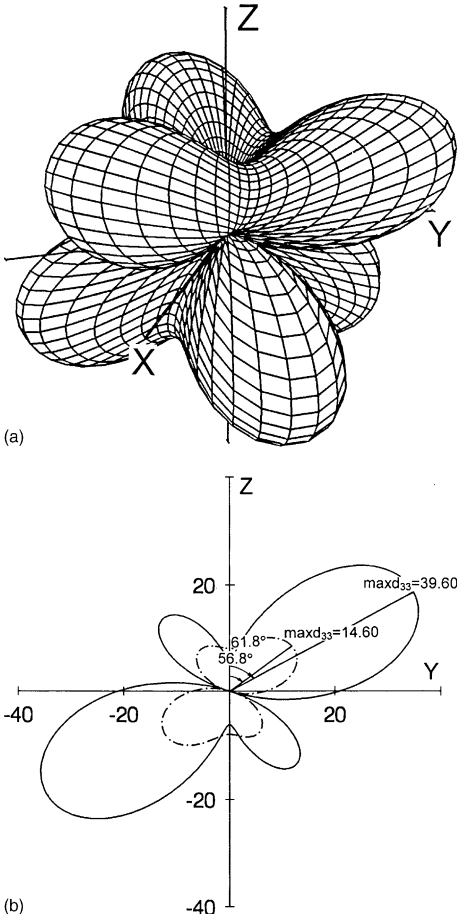

Fig. 1. (a) Schematic diagram of piezoelectric constant d_{33} drawn by the experimental data of $LiNbO_3$. (b) Piezoelectric constant d_{33} of $LiNbO_3$ and $LiTaO_3$ in *YOZ* plane (unit: pC/N): (—) $LiNbO_3$ (-·-·-) $LiTaO_3$.

from which the symmetry of 3 m point group can be cleanly observed. These schematic diagrams were drawn using they the experimental data on $LiNbO_3$ as shown in Table 1. The interval between the longitude lines and latitude lines is less than 10°. For $LiTaO_3$, the graphs of d_{33} and k_{33} in three-dimensional space exhibit quite similar shapes to

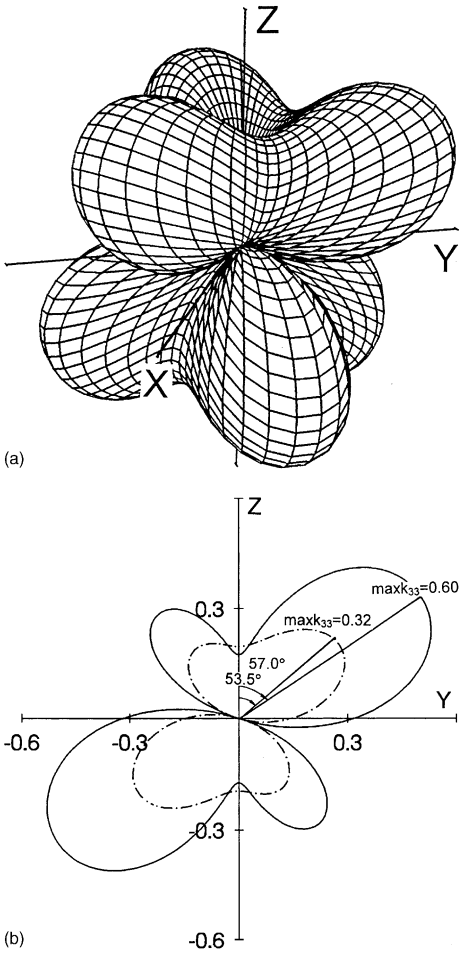

Fig. 2. (a) Schematic diagram of electromechanical coupling factor k_{33} drawn by the experimental data of $LiNbO_3$. (b) Electromechanical coupling factor k_{33} of $LiNbO_3$ and $LiTaO_3$ in *YOZ* plane: (—) $LiNbO_3$ (-·--·-) $LiTaO_3$.

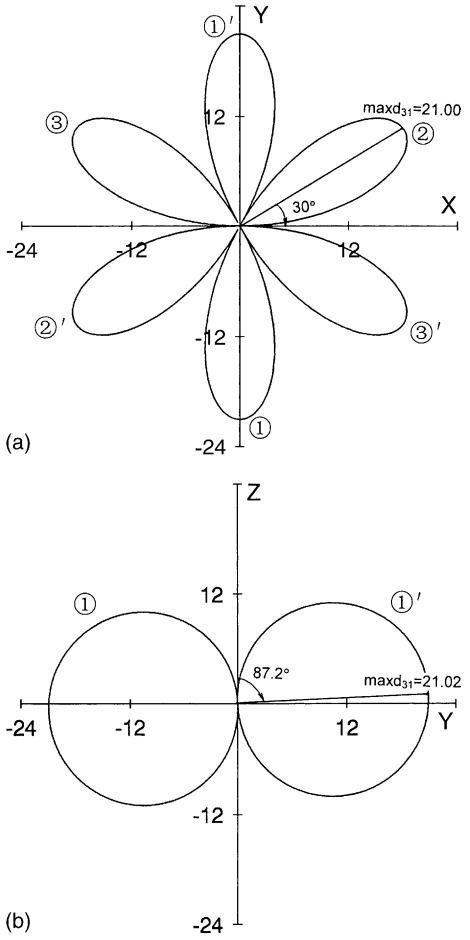

Fig. 3. (a) Schematic diagram of piezoelectric constant d_{31} in XOY plane drawn by the experimental data of $LiNbO_3$. (b) Schematic diagram of piezoelectric constant d_{31} in *YOZ* plane drawn by the experimental data of $LiNbO_3$.

those of $LiNbO_3$, so they are not plotted. Figs. 1(b) and 2(b) show the values of d_{33} and k_{33} for $LiNbO_3$ and $LiTaO_3$ in the *YOZ* plane. The solid line represents $LiNbO_3$ and the dotted line represents $LiTaO_3$. In order to increase the accuracy of determining the optimal directions, the curves are calculated at a reduced step values of 0.1°. For $LiNbO_3$, the maximum values of d_{33} and k_{33} were obtained along directions 61.8° and 57.0° away from the *Z*-axis, respectively. The constant d_{33} of 39.60 pC/N for the canted angle is 6.6 times larger than d_{33} along the *Z*-axis. The factor k_{33} of 0.60 for the canted angle is 3.7 times larger than k_{33} along the *Z*-axis. For $LiTaO_3$, the maximum values of d_{33} and k_{33} were obtained along directions 56.8° and 53.5° away from the *Z*-axis, respectively. The constant d_{33} of 14.60 pC/N for the canted angle is 1.8 times larger than the d_{33} along the *Z*-axis. The factor k_{33} of 0.32 for the canted angle is 1.6 times larger than k_{33} along the *Z*-axis. For these two crystals, the enhancement of d_{33} and k_{33} is remarkably large. From Figs. 1(b) and 2(b), one can see that the piezoelectric effect of $LiNbO_3$ is much stronger than that of $LiTaO_3$.

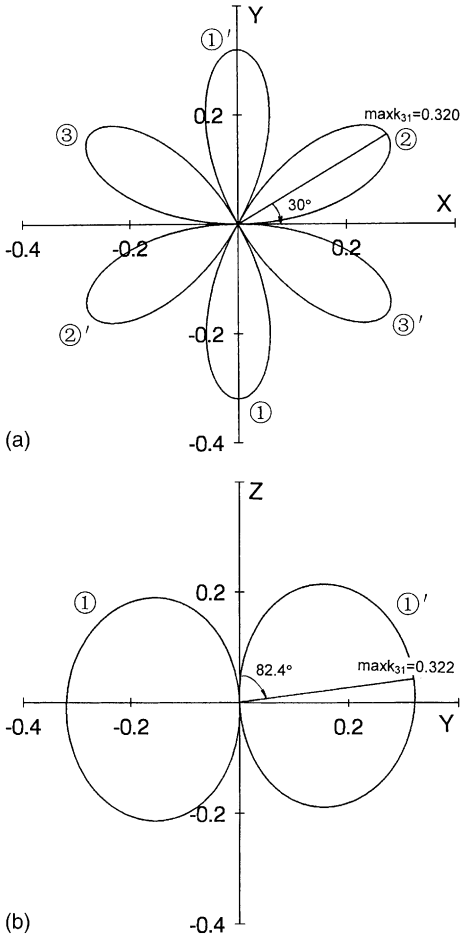

Fig. 4. (a) Schematic diagram of electromechanical coupling factor k_{31} in XOY plane drawn by the experimental data of $LiNbO_3$. (b) Schematic diagram of electromechanical coupling factor k_{31} in *YOZ* plane drawn by the experimental data of $LiNbO_3$.

Figs. 3 and 4 show the schematic diagrams of the orientation dependence of d_{31} and k_{31} projected in the XOY ($\theta = 0$) and *YOZ* ($\varphi = 0$) planes, respectively. These graphs are drawn using the experimental data for $LiNbO_3$; the graphs for $LiTaO_3$ are so similar that they are not plotted here.

From Figs. 3(a) and 4(a), the graphs of d_{31} and k_{31} have six petals in the *XOY* plane. The petals ①, ②, and ③ represent the curves for the three conditions of $0 \leqslant \varphi \leqslant \pi/3$, $2\pi/3 \leqslant \varphi \leqslant \pi$ or $4\pi/3 \leqslant \varphi \leqslant 5\pi/3$, and petals ①′, ②′, and ③′ represent the curves of $d_{31}(\varphi + \pi)$ and $k_{31}(\varphi + \pi)$, which φ satisfies the three conditions above. For $LiNbO_3$, the maximum values of d_{31} and k_{31} are 21.00 pC/N and 0.320, respectively. For $LiTaO_3$, the maximum values of d_{31} and k_{31} are 7.00 pC/N and 0.150, respectively.

From Figs. 3(b) and 4(b), the symbols ① and ①′ correspond to those in Figs. 3(a) and 4(a). For $LiNbO_3$, d_{31} and k_{31} have maximum values of 21.02 pC/N and 0.322, at angles of 87.2° and 82.4° away from *Z*-axis, respectively. For $LiTaO_3$, d_{31} and k_{31} have maximum values of 7.28 pC/N and 0.156, at angles of 74.0° and 72.0° away from *Z*-axis, respectively.

4. Conclusion

The above results show that the piezoelectric properties of single crystals $LiNbO_3$ and $LiTaO_3$ are highly dependent on the crystal orientation, which is related to the symmetry and the structure of these two crystals. This suggests that in order to enhance the piezoelectric properties of specially oriented thin films and single crystals for sensors and some other devices, the optimal directions of $LiNbO_3$ and $LiTaO_3$ should be considered.

Acknowledgement

This work has been supported by the Natural Science Foundation of Beijing Municipality.

References

[1] D.B. Fraser, J. Appl. Phys. 37 (10) (1966) 3853.
[2] A.W. Warner, M. Onoe, G.A. Coqin, J. Acoust. Soc. Am. 42 (6) (1966) 1223.
[3] T. Yamada, N. Niizeki, H. Toyoda, Jpn. J. Appl. Phys. 6 (2) (1967) 151.
[4] T. Yamada, H. Iwasaki, N. Nhzeki, Jpn. J. Appl. Phys. 8 (9) (1969) 1127.
[5] R.A. Graham, Ferroelectrics 10 (1976) 65.
[6] R.A. Graham, J. Appl. Phys. 48 (6) (1977) 2153.
[7] R.S. Weis, T.K. Gaylord, Appl. Phys. A 37 (1985) 191.
[8] Y. Yamashita, Jpn. J. Appl. Phys. Part 1 33 (1994) 5328.

[9] K. Aoki, Y. Fukuda, K. Numata, A. Nishimura, Jpn. J. Appl. Phys. Part 1 33 (1994) 5155.
[10] C.K. Kim, D.S. Yoon, J.S. Lee, C.G. Choi, J. Appl. Phys. 76 (1994) 7478.
[11] X.-H. Du, J. Zheng, K. Uchino, Jpn. J. Appl. Phys. 36 (1997) 5580.
[12] X.-H. Du, J. Zheng, U. Belegundu, K. Uchino, Appl. Phys. Lett. 72 (19) (1998) 2421.
[13] J.F. Nye, Physical Properties of Crystals, Clarendon Press, Oxford, 1979, p. 57.
[14] B.A. Auld, Acoustic Fields and Waves in Solids, John Wiley & Sons, New York, 1973, p. 82.